Enhancement of photocurrent in GaInNAs solar cells using Ag/Cu double-layer back reflector

Timo Aho, Arto Aho, Antti Tukiainen, Ville Polojärvi, Turkka Salminen, Marianna Raappana, and Mircea Guina

Citation: Appl. Phys. Lett. **109**, 251104 (2016); doi: 10.1063/1.4972850
View online: http://dx.doi.org/10.1063/1.4972850
View Table of Contents: http://aip.scitation.org/toc/apl/109/25
Published by the American Institute of Physics

Enhancement of photocurrent in GaInNAs solar cells using Ag/Cu double-layer back reflector

Timo Aho, Arto Aho, Antti Tukiainen, Ville Polojärvi, Turkka Salminen, Marianna Raappana, and Mircea Guina
Optoelectronics Research Centre, Tampere University of Technology, FI-33720 Tampere, Finland

(Received 20 October 2016; accepted 9 December 2016; published online 22 December 2016)

The effect of a Ag/Cu-based double-layer back reflector on current generation in GaInNAs single-junction solar cell is reported. Compared to Ti/Au reflector, the use of Ag/Cu led to a 28% enhancement of short-circuit current density, attaining a value of $\sim$14 mA/cm^2 at AM1.5D (1000 W/m^2) under a GaAs filter. The enhanced current generation is in line with requirements for current-matching in GaInP/GaAs/GaInNAs triple-junction solar cells. The Ag/Cu reflectors also had a low contact resistivity of the order of 10^{-6} Ω·cm^2 and none of the samples exhibited notable peeling of metals in the adhesion tests. Moreover, no discernible diffusion of the metals into the semiconductor was observed after thermal annealing at 200 °C. [http://dx.doi.org/10.1063/1.4972850]

III–V multijunction solar cells are the solution of choice for space and concentrator photovoltaic (CPV) systems, owing to their high power-to-mass ratio, radiation durability, and high efficiency. The continuous progress of multijunction solar cell technology has reached a high level of maturity using approaches involving, e.g., GaInP/GaAs/GaInAs or GaInP/GaAs/Ge designs, which have enabled the efficiencies of over 30% for space[1] and over 40% for CPV.[2] However, these achievements are still far from the theoretical potential, prompting for new approaches to increase the number of junctions for better matching to the solar spectrum.[3] Amongst the recent approaches to increase the efficiency of multi-junction solar cells, the use of lattice-matched $Ga_{1-x}In_xN_yAs_{1-y}$ layers grown by molecular beam epitaxy (MBE) has emerged as very promising design.[4,5] More recently, a combination of MBE and metalorganic chemical vapor deposition (MOCVD) epitaxy was developed as a practical approach to fabricate GaInNAs-based solar cells, exploiting the key features that are established in the production of commercial solar cells.[6] The main advantages offered by GaInNAs rest upon their ability to tailor the bandgap in a wide range from approximately 0.8 eV to 1.42 eV while remaining lattice-matched to GaAs and Ge.[4,7] Despite the recent achievement and good potential for future developments, at high N compositions ($y \geq 0.04$) required for bandgaps below 0.9 eV, the photovoltaic operation of GaInNAs solar cells is reduced due to relatively low charge carrier lifetimes (below 1 ns) leading to short minority carrier diffusion lengths of under $\sim$1 μm, and high p-type background doping of the order of 10^{16} cm^{-3} or higher.[8–10] High background doping level narrows the depletion region, which together with the short diffusion length limits the thickness of an optimized absorption layer, resulting in lower quantum efficiencies.[9–12] To obtain wider depletion regions and higher quantum efficiencies, the p-type background doping should be reduced down to the order of 10^{15} cm^{-3} or below, which still remains a challenging task at high N compositions ($y \geq 0.04$). This issue can be mitigated by adding a reflector on the back side of the solar cell that would allow the use of a thinner absorber with enhanced photogeneration.[13] Highly reflective back surface reflectors effectively double the absorption length in the photogenerating layer. As a result, the charge collection efficiency is improved, which increases the short-circuit current density (J_{sc}).[14] Furthermore, the open circuit voltage (V_{oc}) will theoretically increase as a consequence of higher effective light concentration in the junction and the absorption in average occurs closer to the depletion region, which decreases the nonradiative recombination.[15]

In this paper, we report the operation of a GaInNAs solar cell with a Ag/Cu back surface reflector. Amongst the options for developing non-alloyed back surface reflectors, Ag, Au, and Cu provide almost ideal reflectivity at wavelengths longer than 800 nm.[16] Au as a reflector material[17] is known to be expensive, and therefore, to reduce the solar cell fabrication costs the use of other metals, such as Ag and Cu, would be an attractive alternative. The Ag back reflector has already been reported to work well in GaAs and GaInP solar cells,[18,19] but Ag has not been applied to GaInNAs solar cells. Furthermore, Cu has also been used as a part of the back side contact in GaAs solar cells, but Cu is also known to diffuse easily into III–V semiconductors and thus to reduce the V_{oc}.[20–22] In our approach, we have studied GaInNAs solar cells with double-layer Ag/Cu reflectors exhibiting high reflectance, good adhesion, and low contact resistance. Moreover, a thin Ag layer acts as a diffusion barrier, preventing Cu diffusion into the semiconductor structure even when the cell is subjected to thermal annealing.

Single-junction GaInNAs solar cells were grown by MBE following the process described in Ref. 9. A generic sample structure is presented in Fig. 1. In our benchmark process, as a back contact we used Ti/Au annealed at 420 °C for 90 s to ensure formation of an ohmic contact. Here, we have replaced Ti/Au contact layers with higher-reflectivity metals and fabricated the contact without annealing. Four different metal reflectors were deposited using an electron

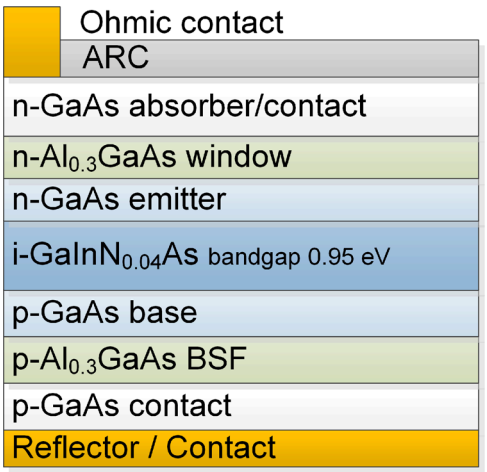

FIG. 1. Generic test structure of the back surface reflector cell. Light enters to the structure from the n-GaAs side.

beam evaporator: Ag/Cu/Ni/Au (denoted as Ag/Cu), Cu/Ni/Au (denoted as Cu), Au (100 nm), and Ti/Au (50 nm/100 nm). Thicknesses of individual layers for the Ag/Cu and Cu samples were: 100 nm for Cu layers, 10 nm for Ni, and 50 nm for Au. Moreover, for the Ag/Cu reflector, we studied three different Ag layers, with thicknesses of 10 nm, 30 nm, and 50 nm. The purpose of Ag is to act as a diffusion barrier for Cu and to provide high reflectance in combination with the Cu layer. The Cu layer acts as a current spreader and conductor. Ni is required between the Au and Cu layers as an adhesion layer and Au acts as a protective layer and bonding surface.

Indium contacts were deposited on the top of the solar cells and the surface was coated with a double-layer TiO_2/SiO_2 antireflection coating by an electron beam evaporator. External quantum efficiency (EQE) measurements were performed with a setup equipped with a 250 W quartz tungsten halogen lamp. The narrow excitation wavelength span for the probe beam was selected by using a Digikrom DK240 monochromator and an 800 nm long-pass filter placed before the monochromator. The signals from the solar cells and from the reference detectors were measured using an SRS SR830 lock-in amplifier and chopped light. A NIST-calibrated Ge reference detector was used for the whole wavelength range of 800–1500 nm.

Fig. 2 shows the EQE results of GaInNAs solar cells with the back reflectors. In addition, the reflectance results of double-side polished semi-insulating GaAs samples with back surface reflectors are shown in Fig. 2 for comparison of the optical properties of the reflectors. The reflectance was measured using a PerkinElmer Lambda 1050 spectrophotometer. For the Au, Ag/Cu, and Cu back reflector cells, EQE was drastically improved compared to reference Ti/Au. The greatest improvement in EQE is observed near the band edge of GaInNAs, where the absorption coefficient decreases and transmission increases; 52% improvement was achieved for the cell with 10 nm Ag/Cu compared to the cell with the Ti/Au reflector. The highest EQE was obtained for the samples with the Ag/Cu reflector, which is a consequence of higher reflectance of the back reflector. This means that the photons that are not absorbed in the first pass are effectively reflected back to the GaInNAs junction. The difference between the 10 nm, 30 nm, and 50 nm Ag/Cu reflectors is small, meaning

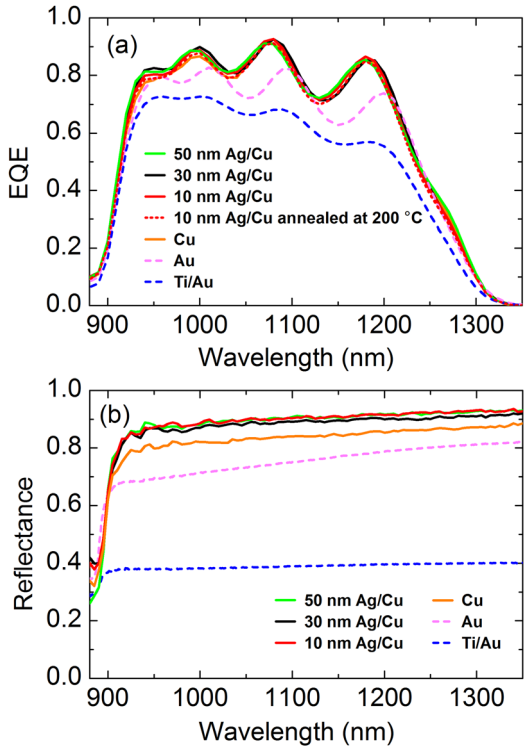

FIG. 2. (a) EQE of the GaInNAs solar cells with various back surface reflectors and (b) the reflectance of double-side polished semi-insulating GaAs samples with back surface reflectors and without ARC. The reflectance was measured through the GaAs from the top side. The correlation between EQE and the reflectance is apparent.

that already a 10 nm layer of Ag is enough to preserve high reflectivity. After thermal annealing at 200 °C for 90 s, the 10 nm Ag/Cu sample maintained high EQE as shown in Fig. 2. This permits that the processing conditions at 200 °C do not adversely affect the functionality of the cell. The EQE of the solar cell with an Au reflector lies between the EQEs of cells with Ag/Cu and Ti/Au back side reflectors. Low EQE of the cell with the Ti/Au reflector can be explained by the fact that the light transmitted through the GaInNAs layer is largely absorbed in the metal layers.

The J_{sc} values at AM1.5G, AM1.5D, and AM0 spectral conditions[23] were deduced from the EQE measurements by integrating over the given spectrum and assuming a thick GaAs filter on top of GaInNAs cell. The results are shown in Table I. The solar cell with the 30 nm Ag/Cu reflector exhibited a J_{sc} value of $\sim$14 mA/cm^2 at AM1.5D (1000 W/m^2), which is 28% higher compared to the reference solar cell with the Ti/Au reflector. These values are similar to the current that can be generated by GaInP/GaAs top cells, which is $\sim$14 mA/cm^2 at AM1.5D (1000 W/m^2).[24] The enhanced photocurrent of the GaInNAs solar cells with the back reflector is proven. This improvement is valid for the bottom junction of a multijunction solar cell. When comparing the conversion efficiency of an optimized GaInP/GaAs/GaInNAs triple-junction solar cell with the Ti/Au back reflector to the cell with the Au/Cu back reflector, 10 percentage points higher efficiency would be reached at $\sim$1000$\times$ AM1.5D resulting in an efficiency of 45% instead of 35%.

Back reflectors that are simultaneously used as ohmic contacts require a low contact resistivity. Conventional ohmic

TABLE I. Measured contact resistivity results and J_{sc} values at AM1.5G (1000 W/m^2), AM1.5D (1000 W/m^2), and AM0 (1366 W/m^2) calculated from the EQE data.

Back Surface Reflector	Contact Resistivity (Ω·cm^2)	J_{SC} AM1.5G (mA/cm^2)	J_{SC} AM1.5D (mA/cm^2)	J_{SC} AM0 (mA/cm^2)
Ti/Au	3×10^{-6}	10.1	10.7	12.7
Au	1×10^{-6}	11.8	12.4	14.8
Cu	4×10^{-6}	12.8	13.4	15.9
10 nm Ag/Cu	4×10^{-6}	12.9	13.6	16.1
10 nm Ag/Cu[a]		12.7	13.3	15.8
30 nm Ag/Cu	4×10^{-6}	13.0	13.7	16.2
50 nm Ag/Cu	5×10^{-6}	13.0	13.7	16.2

[a]Annealed at 200 °C for 90 s

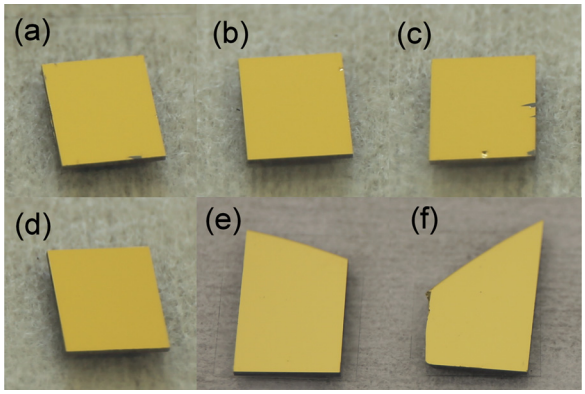

FIG. 3. The samples after the Scotch tape adhesion test. The back surface reflector materials were: (a) 50 nm Ag/Cu, (b) 30 nm Ag/Cu, (c) 10 nm Ag/Cu, (d) Cu, (e) Au, and (f) Ti/Au.

contacts are made of alloyed metals but annealing is shown to lower reflectivity due to the reduction of interface sharpness in comparison to non-alloyed contacts.[25] Although non-alloyed contacts usually suffer from higher contact resistivity,[26] high doping levels can be employed in GaAs to attain low contact resistivity.[20] Typical contact resistivities for p-GaAs are of the order of 10^{-5} Ω·cm^2 for non-alloyed metal contacts and 10^{-7} Ω·cm^2 for alloyed ones.[26,27] The contact resistivity of the Ag/Cu back contact reflectors was measured using the Transmission Line Method (TLM). The contact pads for TLM were fabricated by photolithography onto a separately grown p-type GaAs layer that had a doping level of $\sim 10^{20}$ cm^{-3}. The same metals as for the solar cells were deposited with the electron beam metal evaporator and the mesas were etched using inductively coupled plasma. As presented in Table I, all the reflectors showed low contact resistivity of the order of 10^{-6} Ω·cm^2, which are lower than reported contact resistivities of non-alloyed contacts.[27] These results show that an ohmic contact is formed even without annealing due to high doping in the GaAs layer and high reflectivity of the metal reflector is retained.

Adhesion of the metal reflectors was studied by the Scotch tape peel test.[28] None of the samples showed notable metal peeling, as revealed in Fig. 3. The Au reflector also passed the adhesion test even though Au has been reported to have weak adhesion to GaAs.[20] We observed a small piece of metal peeled off from the sample with 10 nm Ag/Cu as shown in Fig. 3(c). However, this was because of the small cracks on the edge of the sample caused by cleaving. The results indicate that an additional adhesion promoting metal layer, which could reduce the reflectivity, is not needed between the semiconductor and Ag.

The diffusion of Cu and Ag into the semiconductor was investigated by examining the cross-section of the metal-semiconductor interface with a focused ion beam scanning electron microscope (Zeiss Crossbeam 540 FIB-SEM) equipped with an energy-dispersive x-ray spectroscopy detector (EDS) from Oxford Instruments. Samples with similar metals to those for the solar cells were studied. Some of the samples were annealed at 200 °C and 420 °C for 90 s to test the effect of the processing conditions on the atomic diffusion.

The cross-section SEM images and EDS data of the metal-semiconductor interface are presented in Figs. 4 and 5.

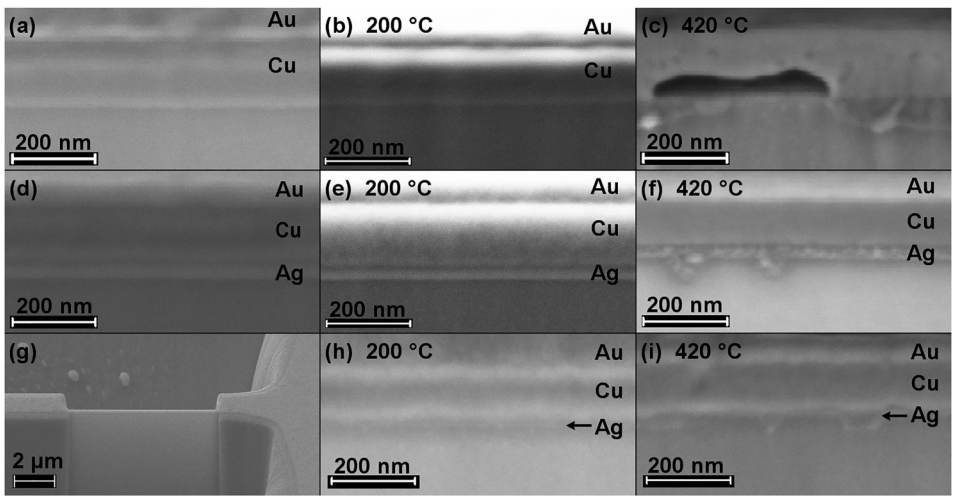

FIG. 4. SEM images of the cross-sections of metals on top of p-GaAs: (a) Cu, (b) Cu annealed at 200 °C, (c) Cu annealed at 420 °C, (d) 50 nm Ag/Cu, (e) 50 nm Ag/Cu annealed at 200 °C, (f) 50 nm Ag/Cu annealed at 420 °C, (g) large scale SEM image of the FIB-processed sample slice to clarify the measurement configuration (10 nm Ag/Cu annealed at 420 °C), (h) 10 nm Ag/Cu annealed at 200 °C, and (i) 10 nm Ag/Cu annealed at 420 °C.

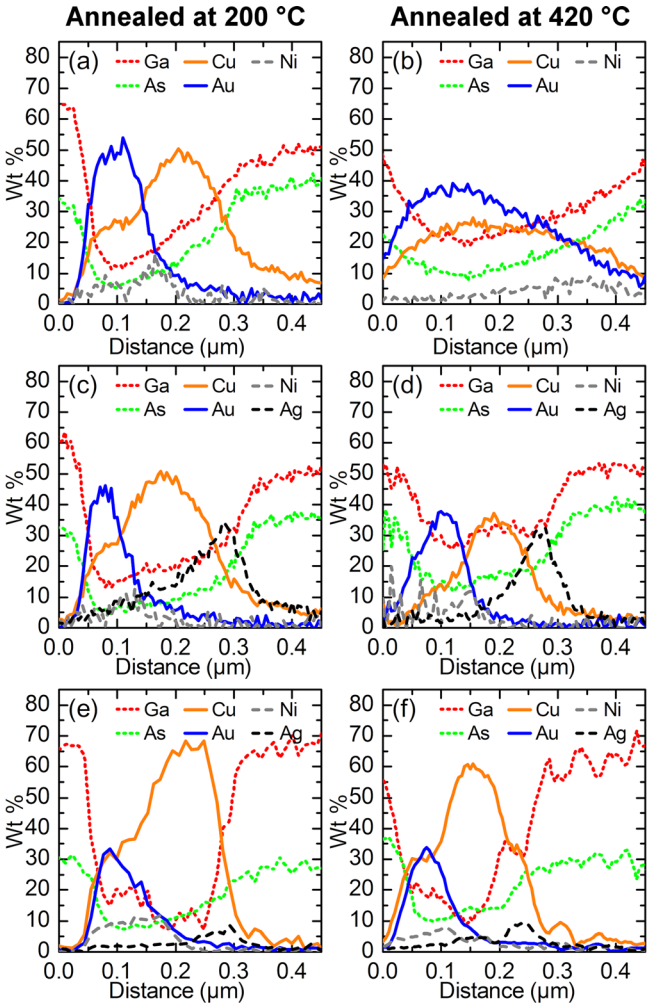

FIG. 5. FIB-EDS results from the cross-section back reflector metals: (a) Cu annealed at 200 °C, (b) Cu annealed at 420 °C, (c) 50 nm Ag/Cu annealed at 200 °C, (d) 50 nm Ag/Cu annealed at 420 °C, (e) 10 nm Ag/Cu annealed at 200 °C, and (f) 10 nm Ag/Cu annealed at 420 °C. The measurement starts from the surface of the sample and the distance on the x-axis represents the depth from the surface. The artefact signals of Ga and As at the surface originate from the electrons hitting the GaAs behind the sample slice made by FIB. The Ga signal is overemphasized due to Ga bombardment during the FIB. Samples were tilted during the measurement, which causes some inaccuracy to the distance.

Cu, Ni, and Au layers remained separated in the non-annealed Cu sample and in Cu sample annealed at 200 °C (Figs. 4(a) and 4(b)). This is also seen in the EDS data (Fig. 5(a)). However, in the SEM image for the sample annealed at 200 °C, the Cu-semiconductor interface is slightly blurred indicating that gradual mixing occurs. In the sample annealed at 420 °C (Fig. 4(c)), a clear mixing of metals and semiconductor was apparent in the SEM image and voids had been formed at the metal-semiconductor interface. Moreover, a color change of the sample surface was observed upon annealing at 420 °C, which is ascribed to alloy formation between Au and Cu.[29] In addition, the mixing of Au and Cu at 420 °C was also seen in EDS data presented in Fig. 5(b), in which Au and Cu peaks are clearly overlapping and the signals finally attenuate in the GaAs layer revealing Cu diffusion to GaAs. Consequently, according to the results, Cu as such is not suitable for the back surface reflector.

The SEM image of the non-annealed 50 nm Ag/Cu sample (Fig. 4(d)) showed that the Ag, Cu, Ni, and Au layers remained well separated and no diffusion occurred even after annealing at 200 °C (Fig. 4(e)). After annealing the 50 nm Ag/Cu sample at 420 °C (Fig. 4(f)), the layers are still separated but Ag has formed triangular spikes into GaAs. The EDS data, in Figs. 5(c) and 5(d), for the samples annealed at 200 °C and 420 °C, did not show mixing of Ag and GaAs, as indicated by the SEM images. Similar behavior was observed for the 10 nm Ag/Cu samples (Figs. 4(h), 4(i), 5(e), and 5(f)). Consequently, even 10 nm of Ag acts as an effective diffusion barrier for Cu and GaAs enabling process temperatures of at least 200 °C.

In conclusion, we have demonstrated the applicability of a double-layer Ag/Cu back contact reflector to enhance the EQE of the GaInNAs solar cell. The solar cell with the 30 nm Ag/Cu reflector resulted in the calculated J_{sc} of $\sim$14 mA/cm^2 at AM1.5D (1000 W/m^2) under a GaAs filter. This value is 28% higher than that for the reference Ti/Au reflector. Furthermore, the adhesion tests showed no notable peeling of metals and the contact resistivity values were of the order of 10^{-6} Ω·cm^2. Moreover, the reflector withstands annealing temperatures of at least 200 °C. The results enable current-matching for GaInNAs materials with a high amount of N corresponding to bandgaps below 0.9 eV, ultimately allowing the development of lattice-matched solar cells with more than three junctions.

The research work of T. A. has been partially financed by European Union via Horizon 2020 research and innovation programme under Grant Agreement No. 687253. Additionally, T.A. acknowledges Ulla Tuominen Foundation and Jenny and Antti Wihuri Foundation for the financial support. The authors wish to thank Riku Isoaho, Jussi-Pekka Penttinen, and Joel Salmi for their technical support.

[1]S. Bailey, J. McNatt, R. Raffaelle, S. Hubbard, D. Forbes, L. Fritzenmeier, and W. Maurer, in *2009 IEEE 34th Photovoltaic Specialists Conference (PVSC), Philadelphia, PA, USA* (IEEE, 2009), pp. 001909–001913.
[2]M. A. Green, K. Emery, Y. Hishikawa, W. Warta, and E. D. Dunlop, Prog. Photovoltaics Res. Appl. **24**, 905 (2016).
[3]A. Luque, J. Appl. Phys. **110**, 031301 (2011).
[4]D. B. Jackrel, S. R. Bank, H. B. Yuen, M. A. Wistey, J. S. Jr. Harris, A. J. Ptak, S. W. Johnston, D. J. Friedman, and S. R. Kurtz, J. Appl. Phys. **101**, 114916 (2007).
[5]M. A. Green, K. Emery, Y. Hishikawa, W. Warta, and E. D. Dunlop, Prog. Photovoltaics Res. Appl. **21**, 1 (2013).
[6]A. Tukiainen, A. Aho, G. Gori, V. Polojärvi, M. Casale, E. Greco, R. Isoaho, T. Aho, M. Raappana, R. Campesato, and M. Guina, Prog. Photovoltaics Res. Appl. **24**, 914 (2016).
[7]D. J. Friedman, J. F. Geisz, S. R. Kurtz, and J. M. Olson, in *2nd World Conference and Exhibition on Photovoltaic Solar Energy Conversion, Vienna, Austria* (European Commission, 1998), pp. 6–10.
[8]A. J. Ptak, D. J. Friedman, S. R. Kurtz, and R. C. Reedy, J. Appl. Phys. **98**, 094501 (2005).
[9]A. Aho, V. Polojärvi, V.-M. Korpijärvi, J. Salmi, A. Tukiainen, P. Laukkanen, and M. Guina, Sol. Energy Mater. Sol. Cells **124**, 150 (2014).
[10]A. Gubanov, V. Polojärvi, A. Aho, A. Tukiainen, N. V. Tkachenko, and M. Guina, Nanoscale Res. Lett. **9**, 80 (2014).
[11]V. Polojärvi, A. Aho, A. Tukiainen, A. Schramm, and M. Guina, Appl. Phys. Lett. **108**, 122104 (2016).
[12]V. Polojärvi, A. Aho, A. Tukiainen, M. Raappana, T. Aho, A. Schramm, and M. Guina, Sol. Energy Mater. Sol. Cells **149**, 213 (2016).
[13]D. Redfield, Appl. Phys. Lett. **25**, 647 (1974).
[14]J. J. Schermer, G. J. Bauhuis, P. Mulder, E. J. Haverkamp, J. Van Deelen, A. T. J. Van Niftrik, and P. K. Larsen, Thin Solid Films **511–512**, 645 (2006).
[15]O. D. Miller, E. Yablonovitch, and S. R. Kurtz, IEEE J. Photovoltaics **2**, 303 (2012).

[16]M. J. Weber, *Handbook of Optical Materials* (CRC Press, 2002).
[17]T. Aho, A. Aho, A. Tukiainen, V. Polojarvi, J.-P. Penttinen, M. Raappana, and M. Guina, in *2015 IEEE 42nd Photovoltaic Specialist Conference (PVSC), New Orleans, LA, USA* (IEEE, 2015), pp. 1–4.
[18]C. Tsai, G. Liu, G. Fan, and Y. Lee, Solid-State Electron. **54**, 541 (2010).
[19]N. Vandamme, C. Hung-Ling, A. Gaucher, B. Behaghel, A. Lemaitre, A. Cattoni, C. Dupuis, N. Bardou, J. Guillemoles, and S. Collin, IEEE J. Photovoltaics **5**, 565 (2015).
[20]A. G. Baca and C. I. H. Ashby, in *Fabrication of GaAs devices* (IET, London, United Kingdom, 2005), pp. 200–211.
[21]R. H. van Leest, G. J. Bauhuis, P. Mulder, R. van der Heijden, E. Bongers, E. Vlieg, J. J. Schermer, and J. J. Schermer, Sol. Energy Mater. Sol. Cells **140**, 45 (2015).
[22]R. H. van Leest, K. de Kleijne, G. J. Bauhuis, P. Mulder, H. Cheun, H. Lee, W. Yoon, R. van der Heijden, E. Bongers, E. Vlieg, and J. J. Schermer, Phys. Chem. Chem. Phys. **18**, 10232 (2016).
[23]ASTM G173-03, *Standard Tables for Reference Solar Spectral Irradiances: Direct Normal and Hemispherical on 37° Tilted Surface* (ASTM International, 2008).
[24]A. Aho, A. Tukiainen, V. Polojärvi, and M. Guina, Nanoscale Res. Lett. **9**, 61 (2014).
[25]G. J. Bauhuis, P. Mulder, E. J. Haverkamp, J. C. C. M. Huijben, and J. J. Schermer, Sol. Energy Mater. Sol. Cells **93**, 1488 (2009).
[26]G. Stareev, H. Künzel, and G. Dortmann, J. Appl. Phys. **74**, 7344 (1993).
[27]I. G. Akdogan and M. A. Parker, Electrochem. Solid-State Lett. **8**, G106 (2005).
[28]K. Kuwahara, H. Hirota, and N. Umemoto, in *Adhesion Measurement of Thin Films, Thick Films, And Bulk Coatings* (ASTM Special Technical Publication, Philadelphia, PA, 1978), pp. 198–231.
[29]H. Okamoto, D. J. Chakrabarti, D. E. Laughlin, and T. B. Massalski, J. Phase Equilib. **8**, 454 (1987).